On the Impact of Probabilistic Shaping on SNR and Information Rates in Multi-Span WDM Systems

Tobias Fehenberger[(1)], Alex Alvarado[(2)], Georg Böcherer[(1)], and Norbert Hanik[(1)]

[(1)] *Institute for Communications Engineering, Technical University of Munich (TUM), 80333 Munich, Germany*
[(2)] *Optical Networks Group, University College (UCL) London, E&EE Department, London, UK*
tobias.fehenberger@tum.de

Abstract: Numerical simulations and the EGN model show that probabilistic shaping decreases SNR due to modulation-dependent nonlinear effects. This SNR loss, however, is less important than the rate increase from shaping, resulting in an overall gain.

OCIS codes: (060.2330) Fiber optics communications, (060.4080) Modulation.

1. Introduction

The data rates of many optical fiber systems are limited by the nonlinear interference (NLI) between neighboring wavelength-division multiplexing (WDM) channels and within the channel of interest. To better understand the effects of NLI on the system performance, Gaussian noise (GN) models have been developed. In the classic GN model [1], NLI is treated as additive noise that follows a circularly symmetric (c.s.) Gaussian distribution and does not depend on the channel input. This was later shown in [2] to be an inaccurate simplification, and enhanced GN (EGN) models have been presented [2, 3] that give a more accurate representation of modulation-dependent NLI.

Variations in the input modulation have recently become popular in the context of probabilistic shaping, which has been demonstrated to enable improved sensitivity, spectral efficiency, and reach in optical communication systems [4]. Most of the work on shaping uses input distributions that are optimized for a linear additive white Gaussian noise (AWGN) channel, and the effects of probabilistic shaping on NLI have largely been ignored.

In this paper, we extend our previous work [5] to study how shaping affects the signal-to-noise ratios (SNRs) and the achievable information rates (AIRs) of an optical communication system with shaped 64QAM and 256QAM input. In our analysis, we use the EGN model and extensive split-step Fourier method (SSFM) simulations to show that shaping leads to an SNR decrease but simultaneously increases AIRs. To the best of our knowledge, this is the first study of the modulation-dependence of NLI for probabilistically shaped 64QAM and 256QAM input.

2. Probabilistic Shaping

Consider a discrete channel input X with probability mass function (PMF) $P_X(x)$, $x \in \mathscr{X}$, and the corresponding output Y of a complex AWGN channel with noise variance σ_n^2. The optimal input distribution P_X^* is SNR-dependent, and we use a Maxwell-Boltzmann (MB) PMF of the form [6, Sec. III]

$$P_X^*(x_i) = \frac{1}{\sum_{j=1}^{|\mathscr{X}|} e^{-\nu|x_j|^2}} e^{-\nu|x_i|^2}, \quad \frac{\mathbb{E}[|\rho X|^2]}{\sigma_n^2} \triangleq \mathrm{SNR}, \tag{1}$$

where ν and ρ are scalars that are chosen such that the AIR is maximized for the considered SNR. A bit-metric decoding rate [5, Sec. II-A] is used as AIR for bit-wise decoders. For this optimization problem of finding the shaped input, we must differentiate between two SNRs. The *shaping SNR* is used at the transmitter to perform the shaping optimization, while the *channel SNR* is the SNR of the actual channel, as shown in Fig. 1. Ideally, these two values are identical as we wish to have the input PMF optimized for the channel we transmit over. However, in practical systems, the channel SNR may be unknown at the transmitter, leading to a discrepancy of shaping SNR and channel SNR. As a result, a suboptimal input PMF would be used. In this work, shaping SNR as a figure of merit allows us to describe with a single parameter how strongly the input is shaped. For increasing shaping SNRs, the optimized input PMF tends to a uniform distribution; a smaller shaping SNR means that the input is shaped more strongly.

3. The GN and EGN Model

The effective channel SNR, $\mathrm{SNR}_{\mathrm{eff}}$, of a signal after propagation over an optical fiber channel and after receiver digital signal processing (DSP) can be written as [5, Sec. III]

$$\mathrm{SNR}_{\mathrm{eff}} = \frac{P_{\mathrm{tx}}}{\sigma_{\mathrm{eff}}^2} = \frac{P_{\mathrm{tx}}}{\sigma_{\mathrm{ASE}}^2 + \sigma_{\mathrm{NLI}}^2} = \frac{P_{\mathrm{tx}}}{\underbrace{\sigma_{\mathrm{ASE}}^2 + P_{\mathrm{tx}}^3 \cdot \chi_0}_{\text{GN+EGN: modulation-independent}} + \underbrace{P_{\mathrm{tx}}^3 \left[(\hat{\mu}_4 - 2) \cdot \chi_4 + (\hat{\mu}_4 - 2)^2 \cdot \chi_4' + \hat{\mu}_6 \cdot \chi_6\right]}_{\text{EGN only: modulation-dependent}}}, \tag{2}$$

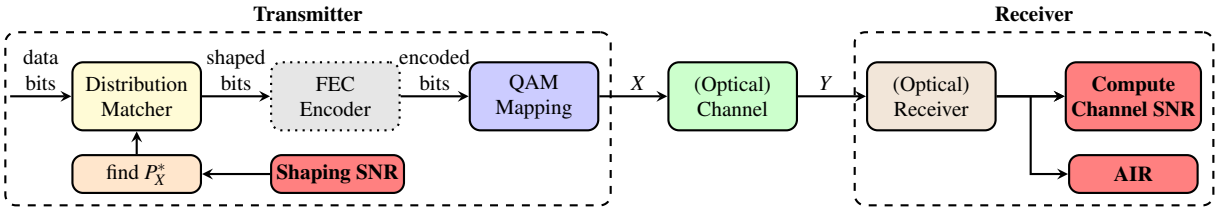

Fig. 1. Block diagram of the shaped communication system. The FEC encoder is omitted in the considered setup as we focus on SNRs and AIRs. The shaping SNR required to find the optimal input P_X^* as well as the channel SNR and AIR (both computed at the receiver) are highlighted in red.

where P_{tx} is the optical launch power, σ^2_{ASE} the amplified spontaneous emission (ASE) noise variance from the optical amplifiers, and σ^2_{NLI} is the NLI variance that includes both intra- and inter-channel distortions. The difference between the classic GN model and the EGN model lies in the term σ^2_{NLI}. With the EGN models [2, 3], we can split σ^2_{eff} into a modulation-independent and a modulation-dependent term, as shown in (2). Only the first NLI summand is included in both models. The second term reduces the NLI variance for finite QAM and is approximately zero for Gaussian input. This modulation-dependence is described by the real-valued scalars χ_4, χ_4', and χ_6, which are the coefficients that represent the contributions of the fiber nonlinearities, and by the k^{th} moment $\hat{\mu}_k$ of the channel input X, which is defined as $\hat{\mu}_k = \mathbb{E}[|X|^k]$ for symmetric and unit-energy X. For QAM input that is shaped according to (1), a stronger shaping leads to increased $\hat{\mu}_4$ and $\hat{\mu}_6$, whereas a uniform input minimizes these moments. In the context of (2), this means that the EGN model predicts an SNR decrease for shaped input compared to a uniform constellation.

In this work, the effective channel SNR of the GN model is obtained from closed-form expressions for a multi-span non-Nyquist WDM system [1, Sec. XI] that include coherent NLI accumulation. The EGN coefficients are computed via Monte Carlo integration over 1 million samples [7, Appendix]. Note that four-wave mixing effects were neglected due to their minor contribution to the overall NLI for the considered system.

4. Simulation Setup and Parameters

A dual-polarization optical fiber system with 9 WDM channels is simulated. At a symbol rate of 28 GBd, a distribution matcher followed by a QAM mapper generates 250000 MB-shaped 64QAM and 256QAM symbols that are optimized for a particular shaping SNR. A block diagram illustrating the shaping method is shown in Fig. 1. After a root-raised-cosine filter with 1% roll-off, the signal is ideally converted into the optical domain. Uncorrelated WDM neighbors with a different data sequence of the same shaped QAM format are generated and added in the frequency domain at a 30 GHz WDM spacing. The launch power per channel is always -1 dBm, which is found to be the optimum in all considered cases within a 1 dB granularity. The fiber link has 8 spans for 256QAM and 20 spans for 64QAM. Each span consists of 100 km standard single-mode fiber (α=0.2 dB/km, γ=1.3 $\frac{1}{\text{W}\cdot\text{km}}$, D=17 ps/nm/km), followed by an optical amplifier with 4 dB noise figure. The signal propagation is simulated using the SSFM with 0.1 km step size and 32 samples per symbol. At the receiver, the center channel, which is the channel under test, is band-pass filtered and chromatic dispersion is compensated. After a matched filter, the channel SNR is estimated from the output samples as an average over both polarizations. The total AIR in bits per 4D-symbol (bit/4D-sym) is computed from the output samples as the sum of the per-polarization AIRs, which are obtained with c.s. Gaussian statistics.

5. Results

Figure 2 (a) shows the channel SNR versus shaping SNR for 64QAM over 2000 km. For the SSFM simulations (markers), the shaping SNR is varied at the transmitter in steps of 0.1 dB, giving a total of 100 SSFM simulation runs. Although the SSFM results fluctuate slightly due to their Monte Carlo nature, a clear trend can be observed: for stronger shaping, i.e., smaller shaping SNRs, the channel SNR decreases. The slope and also the absolute values of the EGN channel SNRs (red solid line) match the simulations accurately, which confirms that *shaping decreases SNR*. The GN model (green dashed line), however, incorrectly predicts a constant channel SNR as it does not include the channel input statistics. For the AIRs shown in Fig. 2 (b), the simulations and the EGN model perfectly match each other. Both AIR curves demonstrate that the shaping method of (1), despite the reduction in channel SNR, leads to AIR improvements. The maximum shaping gain over uniform 64QAM, which has an AIR of 8.86 bit/4D-sym (not shown in Fig. 2 (b)), is 0.4 bit/4D-sym. We observe that variations of a few dB around the optimal shaping SNR lead to an only slightly decreased shaping gain, showing the robustness of the AIRs to a suboptimal input.

The GN model in Fig. 2 finds a different optimum shaping SNR and a different maximum AIR. Somewhat unexpected, the GN model gives higher channel SNRs and larger AIRs than EGN for a wide range of shaping SNRs,

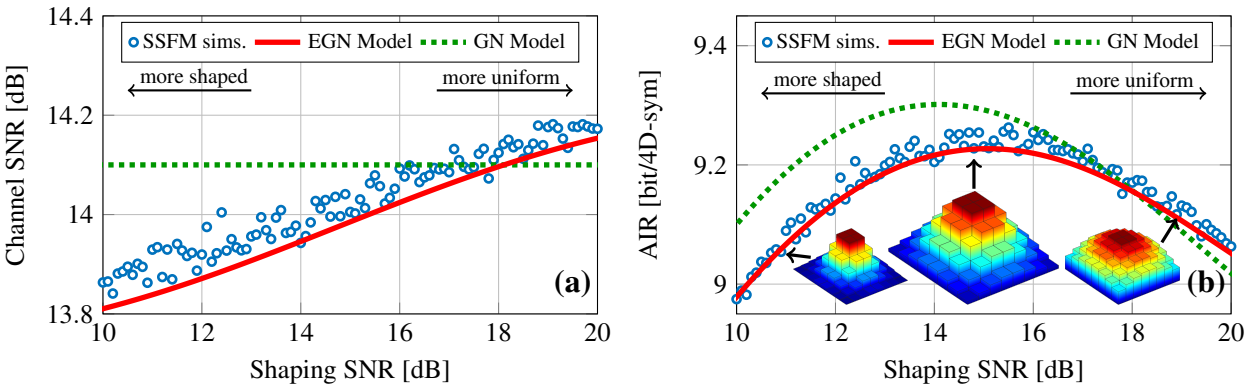

Fig. 2. Channel SNR (a) and AIR in bit/4D-sym (b) versus shaping SNR for 64QAM over 2000 km. The channel SNR for uniform 64QAM simulations is 14.2 dB, corresponding to an AIR of 8.86 bit/4D-sym. The insets in (b) show the optimized PMFs at shaping SNRs of 11 dB, 15 dB, and 19 dB (left to right).

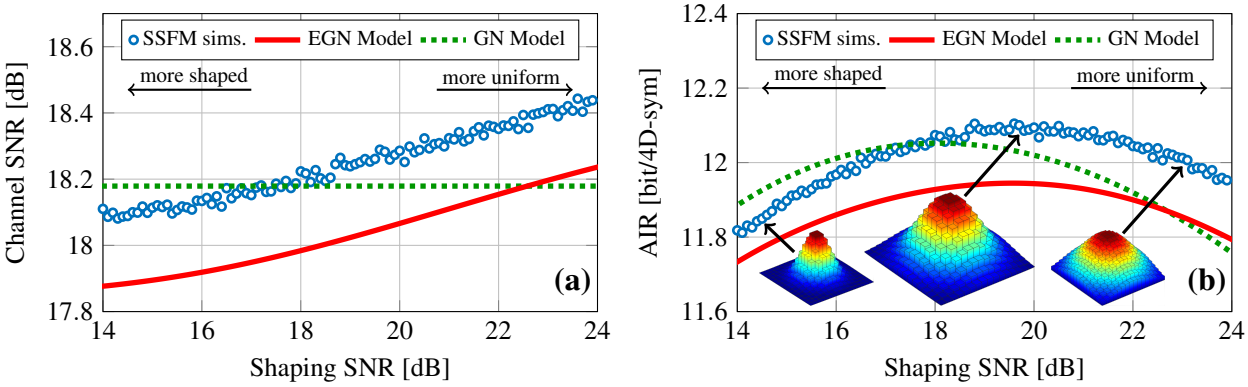

Fig. 3. Channel SNR (a) and AIR in bit/4D-sym (b) versus shaping SNR for 256QAM over 800 km. For uniform 256QAM simulations, the channel SNR is 18.5 dB, and the AIR is 11.5 bit/4D-sym.

although the EGN model in (2) predicts a decrease in NLI variance and thus better performance for QAM input. The small difference of at most 0.3 dB is attributed to the approximations that are necessary for the closed-form expressions of the GN model. We note that the gap between the two models is also present for uniform QAM input.

The channel SNRs for 256QAM over 800 km are shown in Fig. 3 (a). The EGN model correctly reflects that shaping decreases SNR. However, a constant offset of at most 0.2 dB SNR to the simulations is observed, which corresponds to a relative error of less than 5%. The AIRs in Fig. 3 (b) show that the EGN model captures the slope of the simulations and also finds the optimal shaping SNR, yet has an offset that is similar to Fig. 3 (a). We note that in further simulations (not shown), a similar offset is found for uniform 256QAM at this distance, suggesting that the reason for this gap is not how the EGN model includes modulation-dependence. Rather, SSFM simulations of uniform 256QAM over various link lengths indicate that the EGN model under- and then overestimates the simulation SNRs with increasing distance. Further investigations of other QAM formats and setups are required to analyze this aspect thoroughly.

6. Conclusions

We have shown that the EGN model correctly predicts certain characteristics of the nonlinear fiber channel for MB-shaped input: a deviation from uniform input leads to an SNR reduction. AIRs, however, can be increased by using a nonuniform input even though the SNR is reduced, emphasizing the importance of using the correct figure of merit. In the future, the EGN model could be used to obtain shaped distributions that are tailored to the fiber channel. These channel inputs can lead to even larger shaping gains by finding the optimal trade-off between shaping gain on one hand and shaping penalty from enhanced NLI terms on the other.

References

1. P. Poggiolini *et al.*, "The GN model of non-linear propagation in uncompensated coherent optical systems," JLT **30**(24), 2012.
2. R. Dar *et al.*, "Properties of nonlinear noise in long, dispersion-uncompensated fiber links," Optics Express **21**(22), 2013.
3. A. Carena *et al.*, "EGN model of non-linear fiber propagation," Optics Express, **22**(13), 2014.
4. F. Buchali *et al.*, "Rate adaptation and reach increase by probabilistically shaped 64-QAM: an experimental demonstration," JLT **34**(7), 2016.
5. T. Fehenberger *et al.*, "On probabilistic shaping of quadrature amplitude modulation for the nonlinear fiber channel," JLT, **34**(22), 2016.
6. G. Böcherer *et al.*, "Bandwidth efficient and rate-matched low-density parity-check coded modulation," IEEE Trans. Comm. **63**(12), 2015.
7. R. Dar *et al.*, "Accumulation of nonlinear interference noise in fiber-optic systems," Optics Express, **22**(12), 2014.